Second International Conference on CFD in the Minerals and Process Industries
CSIRO, Melbourne, Australia
6-8 December 1999

PREDICTION OF TWO-PHASE EROSION-CORROSION IN BENDS

Anthony KEATING and Srdjan NESIC

Department of Mechanical Engineering, University of Queensland, AUSTRALIA

ABSTRACT

Erosion-corrosion is accelerated corrosion following the removal of protective films. In the past, the majority of erosion-corrosion research has been undertaken using experimental methods. Today, numerical methods provide researchers with an additional tool for investigation.

The CFD code PHOENICS has been used to predict hydrodynamic flow fields in a 180° bend and associated mass transfer rates at high Schmidt numbers (Sc = 520) characteristic for corrosion. The k-ε two-equation eddy-viscosity model for turbulence has been used. To allow for integration through the viscous sub-layer, the Lam-Bremhorst low Reynolds number damping functions were used. Hydrodynamic flow fields and mass transfer rates have been verified against experimental results. Mass transfer rates were directly converted into corrosion rates assuming oxygen limiting mass transfer control.

A numerical particle-tracking code has been developed independently in order to predict erosion. The effect of turbulence on particle motion has been accounted for by the use of an eddy interaction model. Tests have been performed on the particle-tracking code to validate the Eulerian statistics. Two erosion models have been integrated into the code and verified against experimental data. Predictions of erosion, corrosion and erosion-corrosion in a three-dimensional square-sectioned U-bend are presented ($Re = 5.67 \times 10^4$, $R_c / D = 3.35$).

NOMENCLATURE

C	concentration of species (mol/m^3)
CR	corrosion rate (mm/yr)
d	mass diffusivity (m/s)
D_h	width of duct (m)
d_p	particle diameter (m)
ER	erosion rate (mm/yr)
k	turbulent kinetic energy (m^2/s^2)
k_m	mass transfer coefficient (m/s)
L_E	eddy length (m)
M	molecular mass (kg/kmol)
m	mass (kg)
p	fluid pressure (Pa)
Q	volume (m^3)
R_c	radius of curvature (m)
Re	Reynolds number, $Re = u_b D_h / \nu$
Sc	Schmidt number, $Sc = \nu / d$
Sh	Sherwood numbers, $Sh = k_m D_h / d$
S_y	Yield strength of material (MPa)
t	time (s)
T_E	eddy lifetime (s)
u	velocity (m/s)

Greek letters

α	particle impact angle (degrees)
ε	dissipation of turbulent kinetic energy (m^2/s^3)
ρ	density (kg/m^3)
τ	shear stress (kg/m^{2}s)
ν	fluid kinematic viscosity (m^2/s)
μ	fluid viscosity (kg/m/s)

Subscripts

b	bulk value
cr	critical value
f	fluid
Fe	iron
p	particle
t	turbulent

INTRODUCTION

Erosion-corrosion, defined as accelerated corrosion following the removal of surface films is a common cause of equipment failure. It can often be assumed that corrosion is under mass transfer control while erosion is controlled by the flow of a second, particulate phase. Both of these processes can be investigated using numerical techniques. Since liquid/particle flow is modeled here, it has been assumed that surface films are easily removed by the particles. This is a valid assumption as corrosion films are brittle-like materials and therefore are eroded easily by impacting particles (Finnie, 1967).

For some time now, computational fluid dynamics (CFD) has been used to predict turbulent fluid flow with some success. However only recent advances in computational power have allowed researchers to use CFD for mass transfer and corrosion studies. The reason for this is as follows: to accurately model mass transfer near solid boundaries, it is necessary to fully resolve the mass transfer boundary layer. In aqueous flows this may be an order of magnitude smaller than the viscous sub-layer. This requires extremely fine grids in the near-wall region. CFD, using fine near-wall grids with correct near-wall turbulence models can therefore provide mass transfer data for corrosive species. If corrosion is assumed to be mass transfer controlled, a simple relationship can be derived between the wall mass transfer coefficient and corrosion rate.

Previously, researchers have been limited to two-dimensional investigations in relatively simple geometry. Investigations of mass transfer in an axi-symmetric sudden expansion have been performed by Runchal (1971), Nesic et. al. (1992) and Herrero et. al. (1994). Mass transfer

predictions in a two-dimensional 90° bend have recently been reported by Bergstrom et. al. (1998). Nesic and Postlethwaite (1991) predicted corrosion (and compared their predictions to experimental results with some success) in an axi-symmetric sudden expansion using the same method presented in the present work.

The modeling of solid, particulate phases can typically be achieved using a Lagrangian description of particle motion. In most CFD simulations, time-averaged mean flow and turbulence quantities are obtained. Through the use of eddy-interaction models, the effect of turbulence on particle motion may be accounted for. A Lagrangian description has a significant advantage over an Eulerian description as detailed wall interaction information can be obtained without additional modeling. Using this information, an erosion model can be used to determine erosion rates.

Wang et. al. (1996) used a simple method of particle tracking, neglecting the effect of turbulence on particle trajectories, to predict sand erosion rates in 90° bends. Nesic (1991) performed simulations of the erosion of stainless steel and erosion-corrosion of mild steel by sand particles. He used an eddy-interaction model to account for the effect of turbulence on the particle paths, which had a significant effect on erosion rates. Nokleberg and Sontvedt (1998) using the commercial CFD code FLUENT and a similar method to Nesic (1991) have successfully predicted sand particle erosion in choke valves. The predictions of Nokleberg and Sontvedt (1998) allowed Norsk Hydro ASA to redesign the valves and reduce erosion rates by factors of 50-100.

Using a combination of mass transfer predictions on fine near-wall grids, and Lagrangian particle tracking with an eddy-interaction model, predictions of erosion-corrosion in relatively complex geometry can be obtained.

OBJECTIVES OF THIS WORK

The primary objective of this work was to investigate erosion-corrosion in bends using currently available computational tools. Previous work has primarily been on two-dimensional geometry. The current work extends this to three-dimensions and includes a number of additional complexities due to the nature of flow in a bend.

HYDRODYNAMIC AND CORROSION MODELS

Standard eddy-viscosity k-ε turbulence model

The commercial CFD code PHOENICS was used for the modeling of fluid flow and mass transfer. As with most modern CFD codes, PHOENICS solves the Reynolds-averaged Navier-Stokes and continuity equations using an eddy-viscosity concept in order to predict fluid flow. The following coefficients in the k-ε turbulent model have been used:

$$\begin{aligned} &C_{\varepsilon 1} = 1.44, \quad C_{\varepsilon 2} = 1.92, \\ &C_{\mu} = 0.09, \quad \sigma_k = 1.0, \\ &\sigma_{\varepsilon} = 1.3 \end{aligned} \tag{1}$$

The pressure-velocity coupling is solved using the SIMPLE algorithm of Patankar and Spalding (1972). Discretization in space was performed using the Leonard's (1979) quadratic upward interpolation (QUICK) scheme.

Turbulent transport of species equation

To model mass transfer of a corrosive species, it is necessary to solve the conservation of species equation. For turbulent flow a Reynolds-averaged conservation of species equation can be obtained:

$$\frac{\partial \rho_f \overline{C}}{\partial t} + \frac{\partial}{\partial x}\left(\rho_f \overline{u}_j \overline{C}\right) = \left[\left(\frac{\mu}{\rho_f Sc} + \frac{\mu_t}{\rho_f Sc_t}\right)\frac{\partial \overline{C}}{\partial x_j}\right] \tag{2}$$

Note that the turbulent species flux term in this equation has been approximated using the concept of turbulent diffusion, in analogy to the eddy-viscosity concept. For the turbulent Schmidt number, Sc_t. Kays and Crawford (1980) suggest a value of 0.9 in the bulk of the flow.

Near-wall boundary conditions

Corrosion in aqueous flows involves species with high Schmidt numbers. This precludes the use of wall functions, as the molecular diffusion controlled sub-layer is embedded deep within the hydrodynamic viscous sub-layer and has to be resolved. Therefore, integration through the viscous sub-layer is required. To achieve this, a low Reynolds number modification of the k-ε turbulence model such as that proposed by Lam and Bremhorst (1981) is needed. The Lam-Bremhorst low Reynolds number modification uses the following damping functions in the eddy-viscosity and dissipation transport equations:

$$\begin{aligned} f_1 &= 1 + \left(\frac{0.05}{f_\mu}\right)^3 \\ f_2 &= 1 - \exp\left(-R_t^2\right) \\ f_\mu &= \left[1 - \exp\left(-0.0165 R_k\right)\right]^2 \times \left(1 + \frac{20.5}{R_k}\right) \end{aligned} \tag{3}$$

and the turbulent Reynolds numbers, R_k and R_t are:

$$R_k = y\sqrt{\frac{k}{v}}, \quad R_t = \frac{k^2}{v\varepsilon} \tag{4}$$

Corrosion model

From the solution of the turbulent transport of species equation, the wall mass transfer coefficient, k_m can be calculated using the method of Nesic (1991). Assuming mass transfer controlled corrosion, the mass transfer coefficient can be converted to a local corrosion rate. For the case of oxygen corrosion consisting of the reactions:

$$\begin{aligned} 2Fe &\rightarrow 2Fe^{++} + 4e^- \\ O_2 + 2H_2O + 4e^- &\rightarrow 4OH^- \end{aligned} \tag{5}$$

which is often mass transfer controlled, the corrosion rate can be obtained from the mass transfer coefficient using the following equation:

$$CR = \frac{2k_m C_{b_{O_2}} M_{Fe}}{\rho_{Fe}} \times 86400 \times 365 \times 10^3 \qquad (6)$$

PARTICULATE PHASE AND EROSION MODEL

Lagrangian description of particle motion

A Lagrangian description of particle motion is based on the equation of motion for a particle surrounded by a liquid or gas (e.g. Maxey, 1993). In most situations, a number of the terms (the pressure gradient, added mass, Basset history and initial velocity terms) in this equation can be neglected. The resulting differential equation can be solved numerically using a method such as Runge-Kutta, however it has been shown that a recurrence formula can be used more efficiently. Durst, et. al. (1984) linearised and solved the equation for short time steps:

$$u_p^{n+1} = u_f - \left(u_f - u_p^n\right)\exp\left(-\frac{\Delta t}{\tau_p}\right) + g\tau_p\left[1 - \exp\left(-\frac{\Delta t}{\tau_p}\right)\right] \qquad (7)$$

Where the particle relaxation time is defined as:

$$\tau_p = \frac{m_p}{3\pi\mu f_p d_p} \qquad (8)$$

The new position of the particle after a short time, Δt, can be calculated using:

$$x_p^{n+1} = x_p^n + \frac{\Delta t}{2}\left(u_p^{n+1} + u_p^n\right) \qquad (9)$$

Using this method, a particle can be tracked through an instantaneous velocity field. However a problem arises in obtaining an instantaneous velocity field. Typical CFD codes solve the Reynolds-averaged Navier-Stokes equations and obtain Reynolds-averaged velocity components and two averaged turbulence quantities, k and ε. It is necessary to convert these averaged fields into instantaneous velocity fields to account for the effect of turbulence on particle motion.

Eddy-interaction model

The use of an eddy-interaction model is a stochastic technique used to reconstruct the instantaneous velocity field. It is assumed that a particle is in continuous interaction with a succession of fluid eddies as it passes through the domain. Inside each of these eddies the velocity experienced by a particle is constant. Eddies have a finite lifetime and length, determined by the local turbulence quantities.

The instantaneous velocity experienced by a particle interacting with an eddy is calculated using the Reynolds-averaged velocity and turbulent kinetic energy. The turbulent kinetic energy can be converted to a fluctuation velocity. The instantaneous velocity inside an eddy is calculated from a Gaussian distribution with a mean equal to Reynolds-averaged velocity and a standard deviation equal to the calculated fluctuation component.

The lifetime (Lagrangian integral time scale), T_E and length (Lagrangian length scale), L_E of an eddy are calculated using the model of Milojevic (1990):

$$T_E = 0.3\frac{k}{\varepsilon}, \quad L_E = T_E\sqrt{\frac{2}{3}k} \qquad (10)$$

The implementation of the eddy-interaction model was done in accordance with Milojevic's (1990) Lagrangian Stochastic-Deterministic (LSD) model of particle motion. The LSD model accounts for both the crossing trajectories effect and non-homogeneous turbulence. As relatively low concentrations of particles were simulated, only one-way fluid-particle coupling was accounted for.

Erosion model

By far the simplest and most commonly used erosion model is that proposed by Finnie et. al. (1967,1978). Finnie et. al. proposed that erosive wear is a direct consequence of the cutting of surfaces by impacting particles. The erosive wear can then be calculated using:

$$Q = 0.5\frac{m_p u_p^2}{4p} f(\alpha) \qquad (11)$$

The function, $f(\alpha)$ was given by Finnie et. al. (1992) to be angle dependant. For $\alpha \le 18.5°$:

$$f(\alpha) = \left(\sin 2\alpha - 3\sin^2\alpha\right) \qquad (12)$$

For larger angles, $\alpha > 18.5°$:

$$f(\alpha) = \frac{1}{3}\cos^2\alpha \qquad (13)$$

While this model has been widely used in literature, Nesic (1991) found that it greatly overpredicted erosion rates in a sudden axi-symmetric pipe expansion. Using ideas from the earlier works of Bergevin (1984) and Bitter (1963a,1963b), Nesic (1991) improved the predictions of Finnie's erosion model through the use of a critical velocity perpendicular to the surface. Below this no erosion would take place, i.e. the elastic limit of the surface material had not been exceeded. He also proposed that it was the difference between this critical velocity and the particle impact velocity that caused erosive wear. Using this, Nesic proposed the following modification of Finnie's erosion model:

$$\left(u_p \sin\alpha\right)_{Finnie} = u_p \sin\alpha - u_{cr} \qquad (14)$$

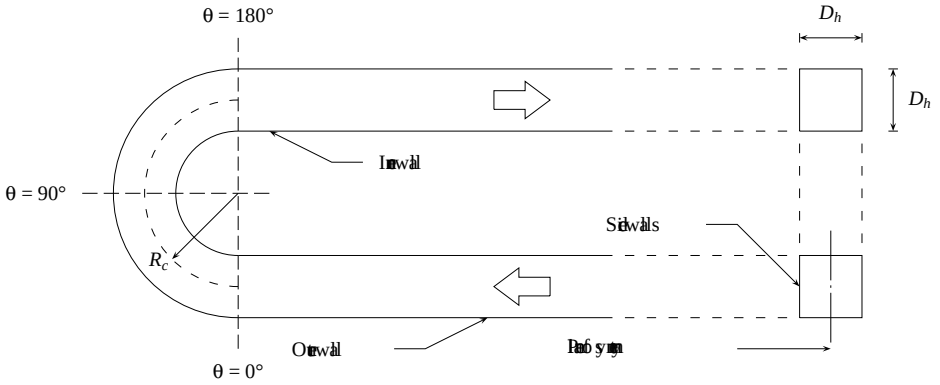

Figure 1: Geometric layout and measuring planes for flow through a three-dimensional square-sectioned U-bend. Includes definitions of inner, outer and side walls as well as the plane of symmetry.

Bitter (1963a,1963b) has reported the critical velocity for a number of materials. For steel, the critical velocity was reported as 0.668 m/s. While erosion models such as those proposed by Bitter (1963a,1963b) and Sundararagan (1991) are more detailed, they are difficult to use due to the number of constants that must be determined empirically.

Implementation

One of the aims of this work was to investigate the use of commercially available CFD tools to predict erosion-corrosion. We were unable to find a package that had the features discussed above. Therefore a custom code was written which interfaced with PHOENICS, and performed particle tracking and erosion prediction.

RESULTS

Verification of the models presented in the previous section was carried out in Keating (1999). During this, a number of problems wee illuminated and are summarised here. Firstly, problems were found to occur in the predictions of mass transfer coefficients. Two reasons were given for this: the variation of turbulent Schmidt number in the near wall region and the use of the Lam-Bremhorst low Reynolds number modification for mass transfer simulations. In the verification of the erosion model, it was found that Finnie's erosion model overpredicted erosion rates. This was corrected by the use of Bergevin and Nesic's modification.

A fully three-dimensional square-sectioned U-bend was simulated and predictions were compared to the measurements of Chang et. al. (1983). A sketch of the domain, including definitions of inner, outer and side walls is given in Figure 1. Table 1 describes the two numerical grids used, WF-A (wall functions used in the near-wall region) and LRN-A (Lam-Bremhorst low Reynolds number model). A comparison between predictions obtained using two different numerical grids and measurements is shown in Figure 2. Predictions are only shown for two measuring planes, 3° and 90° for compactness. Comparisons at other measuring planes are available in Keating (1999). Note that only half of the cross-section was simulated due to a plane of symmetry through the middle of the bend.

	WF-A	LRN-A
Streamwise nodes	96	96
Cross-sectional nodes	10x20	40x80
Total number of nodes	19,200	307,200
Grid expansion factor	1.15	1.15
Wall treatment	WF	LRN
First node wall distance	1095.8μm	6.25μm

Table 1: Numerical grids used for the prediction of single-phase flow in a three-dimensional square-sectioned U-bend. $Re = 5.67 \times 10^4$.

To aid further research in the use of low Reynolds number models it is noted that the use of false time-step relaxation greatly improved convergence for extremely fine near-wall grids.

Relatively good agreement between predictions and measurements can be seen. It is thought that discrepancies that occur in these three-dimensional predictions are due to the isotropic k-ε eddy-viscosity turbulence model. This model seems to only predict secondary motion due to the curvature of the bend. It neglects any effects due to the cross-sectional shape of the duct. This is clearly seen in the reduced magnitude of radial velocity at 90° in the bend.

Mass transfer predictions at a Schmidt number of 520 (for oxygen transport) have been obtained using the above hydrodynamic predictions. A contour plot of predicted Sherwood number on the inner, outer and side walls through the bend is shown in Figure 3. From the mass transfer coefficient predictions, peak film-free oxygen corrosion rates have been calculated and are presented in Table 2. The bulk concentration of oxygen was set to 8ppm. It is shown that the corrosion rate in the bend can increase by a factor of 1.75 compared to fully-developed flow values. While the magnitude of these predictions may be inaccurate due to reasons outlined in the verification study, it is expected that the relative increases and their locations are realistic. This needs to be confirmed experimentally.

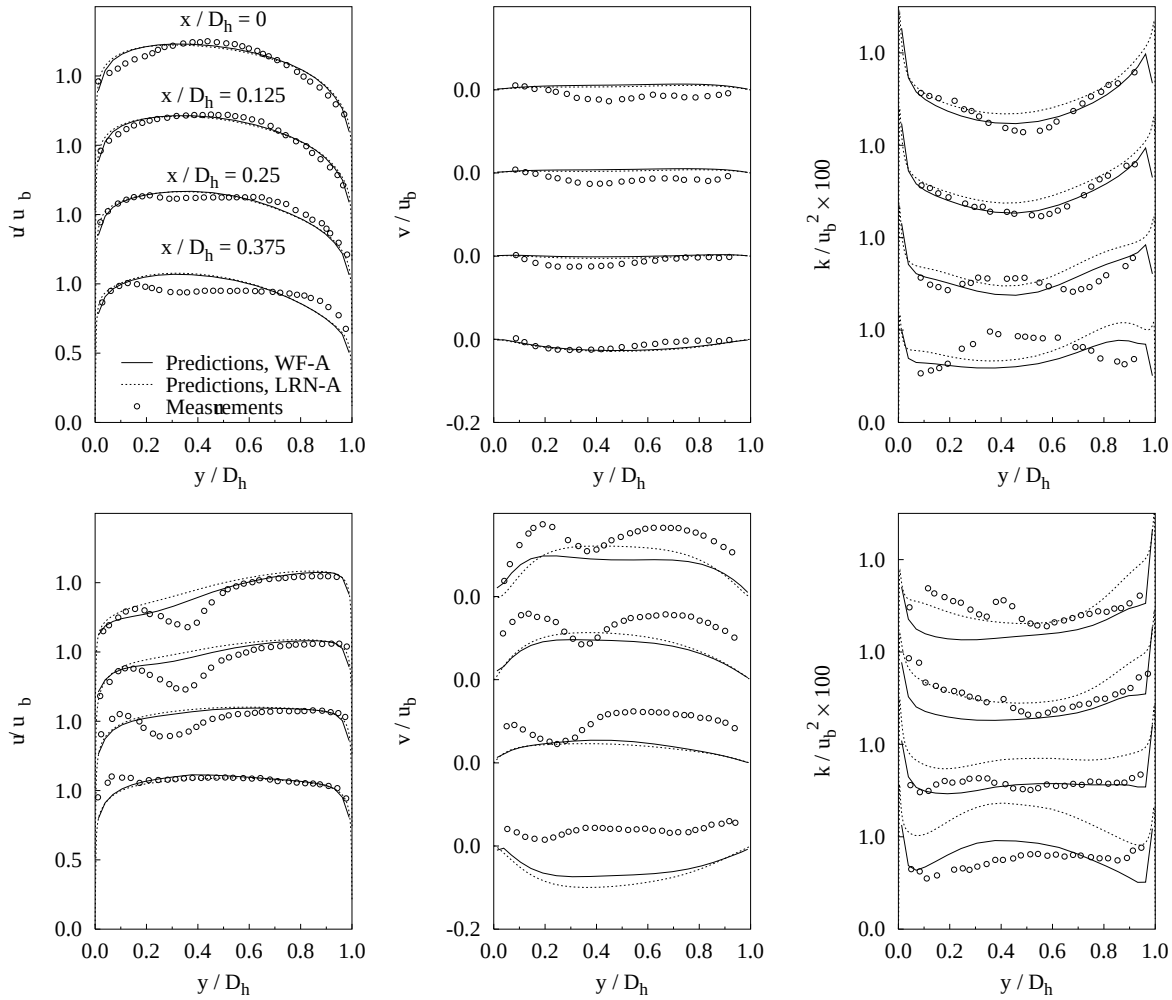

Figure 2: Predictions and mesurements of streamwise velocity, radial velocity and turbulent kinetic energy for flow in a three-dimensional square-sectioned U-bend at a measuring planes at 3° (top) and 90° (bottom) in the bend. Measurements of Chang et. al. (1983). Re = 5.67×10^4. Grid WF-A, wall function coarse grid. Grid LRN-A, Lam-Bremhorst low Reynolds number fine grid. Where x is the distance from the plane of symmetry and y is the distance from the inner wall.

The results from the hydrodynamic simulation were used to compute particle trajectories in the U-bend. Particles were released from a rectangular source at the inlet to the bend. Sand particles (ρ_d = 2700 kg/m^3) with a diameter of 430μm were used. A total of 16,000 particle trajectories were simulated. Simulations were also performed with 32,000 trajectories, but differences in results were less than 5%. Sample particle trajectories (2 trajectories from each of 10 starting locations) for sand particles are given in Figure 4.

A complex balance of three forces influences the motion of particles in the three-dimensional square-sectioned U-bend: gravity, particle inertia and the fluid's primary and secondary velocity. Particles move to either the inner or outer walls due to a balance of particle inertia and gravity, while they are at the same time moved to the side walls due to the fluids secondary motion (neither particle inertia or gravity have any real effect in this plane).

The difference between particle motion in downward and upward facing bends is due to gravity either acting with particle inertia or against it. It is clearly shown that in an upward facing bend, particles impact the outer wall with a greater force that for a downward facing bend.

Erosion rates have been calculated for a 2% sand slurry in a 304A Stainless steel (S_y = 276 Mpa) bend. Contours of erosion rates, calculated using Finnie's erosion model are shown in Figures 5 (downward facing) and 6 (upward facing). Calculations using Bergevin and Nesic's modification resulted in zero erosion rate predictions at this Reynolds number due to the small normal impact velocity of particles. Figure 5 (downward facing bend) shows particles impacting the outer wall at approximately 90° in the bend. From here particles are moved towards the side walls by the secondary motion of the fluid. The peak erosion rate occurs at 180° in the bend. For an upward facing bend (Figure 6), particles impact the outer wall closer to the inlet plane and are then moved to the side walls. The maximum erosion rate occurs closer to the inlet, at 130°.

Peak values of erosion on inner, outer and side walls are given in Table 3. Using the predictions of corrosion and erosion presented above, erosion-corrosion predictions are now presented for the three-dimensional square-sectioned U-bend. The following parameters have been set: 1010A

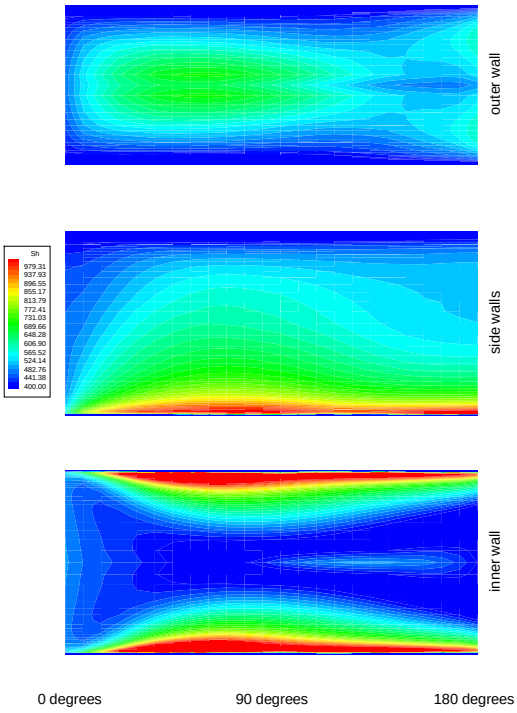

Figure 3: Predictions of Sherwood number for flow through a three-dimensional square-sectioned U-bend. Sc = 520. Re = 5.67 x 10^4.

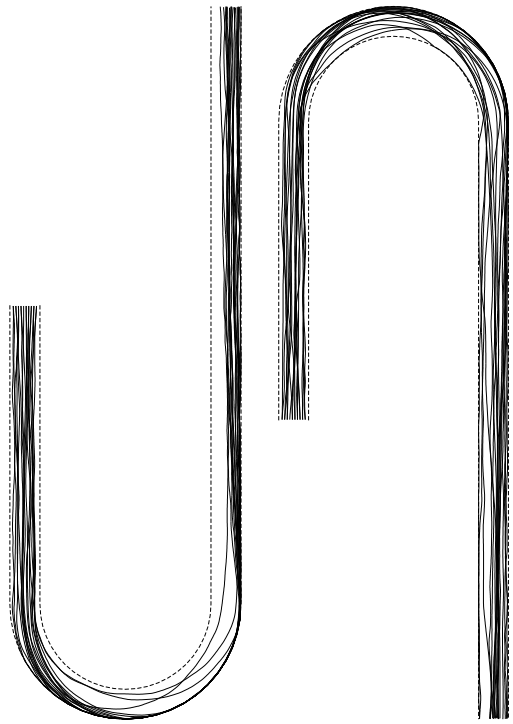

Figure 4: Sample particle trajectories for flow of sand particles in a three-dimensional square-sectioned U-bend. Upward (left) and downward (right) facing bends. Particles enter through the short pipe. Re = 5.67×10^4.

Fully-developed upstream values	
Mass transfer coefficient, $k_m \times 10^5$	2.03
Corrosion rate, CR (mm/yr)	0.12
Peak values on inner wall	
Mass transfer coefficient, $k_m \times 10^5$	5.59
Corrosion rate, CR (mm/yr)	0.33
Position in bend	50°
Distance from centerline (m)	0.0214
Percentage increase	175%
Peak values on outer wall	
Mass transfer coefficient, $k_m \times 10^5$	3.04
Corrosion rate, CR (mm/yr)	0.18
Position in bend	64°
Distance from centerline (m)	0.0054
Percentage increase	50%
Peak values on side walls	
Mass transfer coefficient, $k_m \times 10^5$	4.62
Corrosion rate, CR (mm/yr)	0.27
Position in bend	180°
Distance from inner wall (m)	0.0007
Percentage increase	130%

Table 2: Peak values of film-free single-phase oxygen corrosion rate (mm/yr) on inner, outer and side walls of a three-dimensional square-sectioned U-bend. Re = 5.67×10^4. Sc = 520.

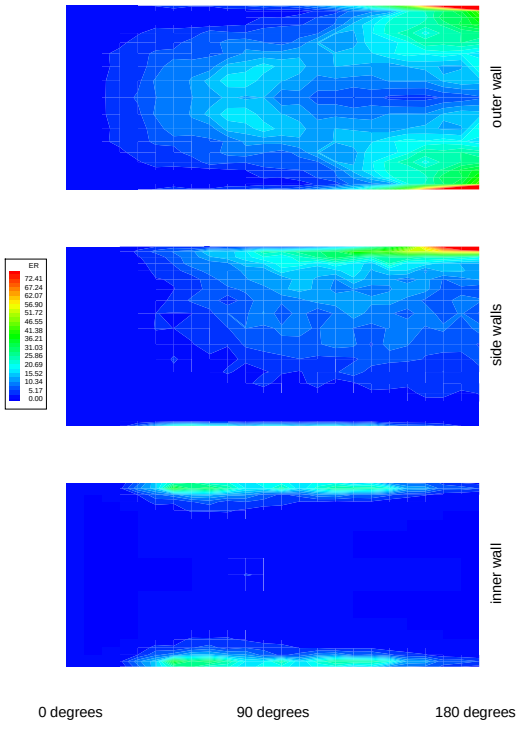

Figure 5: Predictions of erosion rate (mm/yr) for sand particle two-phase flow in a downward facing three-dimensional square-sectioned U-bend. Re = 5.67×10^4.

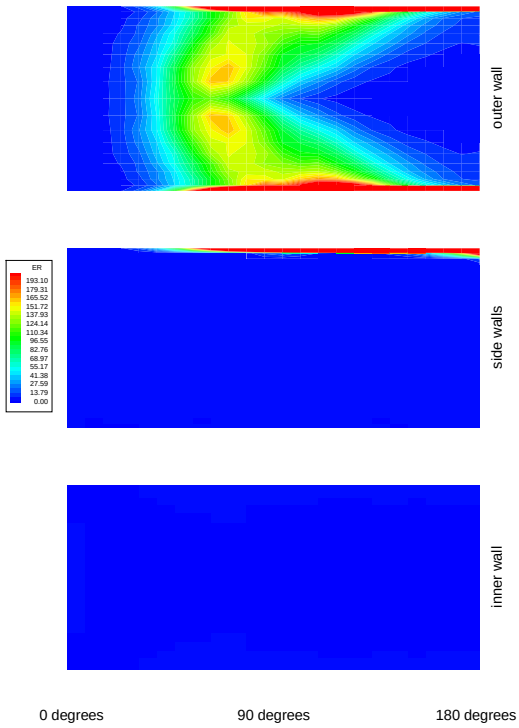

Figure 6: Predictions of erosion rate (mm/yr) for sand particle two-phase flow in an upward facing three-dimensional square-sectioned U-bend. Re = 5.67×10^4.

	downward	upward
Inner wall		
Erosion rate (mm/yr)	36	
Position in bend	50°	
Distance (m)	0.0205	
Outer wall		
Erosion rate (mm/yr)	180	3056
Position in bend	180°	130°
Distance (m)	0.0217	0.0217
Side walls		
Erosion rate (mm/yr)	161	2740
Position in bend	180°	130°
Distance (m)	0.0440	0.0440

Table 3: Predictions of peak erosion rates on inner, outer and side walls of a three-dimensional square-sectioned U-bend. Re = 5.67 × 104. Sand particles, dp = 430μm, volume concentration of 2%. 304A stainless steel base metal. Distance is the distance from centerline of each wall.

carbon steel base metal (S_y = 200 Mpa), sand particles (ρ_p = 2700 kg/m^3, d_p = 430μm) at 2% volume loading and water flow, Re = 5.67×10^4, carrying dissolved oxygen with a bulk concentration of 8ppm. Erosion-corrosion rates at points of maximum erosion and maximum corrosion are given in Tables 4 and 5. Also shown is the percentage of the total damage that is attributed to corrosion. At all points erosion-corrosion was found to be dominated by erosion. The maximum erosion-corrosion occurred at the point of maximum erosion.

	E-CR	%CR
Inner wall		
downward facing (48.75°)	48	0.3%
Outer wall		
downward facing (180°)	244	0.02%
upward facing (131.25°)	4125	<0.01%
Side walls		
downward facing (180°)	220	0.11%
upward facing (131.25°)	3690	<0.01%

Table 4: Predictions of erosion-corrosion rate at points of maximum erosion for two-phase flow in a three-dimensional square-sectioned U-bend. Re = 5.67×10^4. Sand particles, d_p = 430μm, volume concentration of 2%. 1010A carbon steel base metal.

	E-CR	%CR
Inner wall (48.75°)		
downward facing	33	1%
upward facing	2	17%
Outer wall (63.75°)		
downward facing	19	1%
upward facing	220	0.08%
Side walls (180°)		
downward facing	3	11%
upward facing	<1	31%

Table 5: Predictions of erosion-corrosion rate at points of maximum corrosion for two-phase flow in a three-dimensional square-sectioned U-bend. Re = 5.67×10^4. Sand particles, d_p = 430μm, volume concentration of 2%. 1010A carbon steel base metal.

CONCLUSIONS

The present study has used numerical techniques to investigate erosion-corrosion in a three-dimensional square-sectioned U-bend. Hydrodynamic predictions using the commercial CFD code, PHOENICS have been used to predict mass transfer coefficients which have been converted to corrosion rates by assuming mass transfer limiting film-free corrosion. Peak corrosion was found to occur on the inner wall at 50° in the bend. This peak was predicted to be an increase of 175% over fully-developed straight duct flow corrosion rates.

Erosion rates were predicted using flow fields obtained by PHOENICS and imported into a separate particle flow simulation code. The effect of bend orientation was found to have a large effect on particle motion and therefore erosion rates. Peak erosion rates were found to occur at the corner of the outer and side walls near the exit of the bend. Erosion-corrosion was found to be dominated by erosion, with maximum erosion-corrosion rates occurring at points of maximum erosion. The use of Bergevin and Nesic's model to predict erosion rates for flow in a three-dimensional square-sectioned U-bend at Re = 5.67×10^4, resulted in predictions of no erosion. This was due to low normal particle impact velocity. Without experimental results it is impossible to judge if this is correct.

This study shows both the usefulness and the current limitations of numerical tools in the prediction of corrosion, erosion and erosion-corrosion. The lack of

commercially available particle codes required the development of a custom code. However the availability of commercial CFD codes greatly decreased the time required to obtain solutions.

Further research is required in four areas: i) mass transfer and corrosion in three-dimensional geometry (experimental data are missing), ii) investigation of turbulent Schmidt number in the near wall region (recent DNS studies can help here), iii) development of improved k-ε based turbulence models in the near wall region tailored for mass transfer predictions, and iv) development of improved erosion models.

REFERENCES

BERGEVIN, K., (1984), *Effect of slurry velocity on the mechanical and electrochemical components of erosion-corrosion in vertical pipes*, Masters thesis, University of Saskatchewan, Canada.

BERGSTROM, D.J., BENDER, T., ADAMOPOULOS, G. and POSTLETHWAITE, J., (1988), "Numerical prediction of wall mass transfer rates in turbulent flow through a 90° two-dimensional bend", *The Canadian Journal of Chemical Engineering*, **76**, 728—737.

BITTER, J.P.A, (1963a), "A study of erosion phenomena, Part I", *Wear*, **6**.

BITTER, J.P.A., (1963b), "A study of erosion phenomena, Part II", *Wear*, **6**.

CHANG, S.M., HUMPHREY, J.A.C. and MODAVI, A., (1983), "Turbulent flow in a strongly curved U-bend and downstream tangent of square cross-sections", *PhysicoChemcial Hydrodynamics*, **4**, 243—269.

CHENG, G.C., and FAROKHI, S., (1992), "On turbulent flows dominated by curvature effects", *ASME Journal of Fluids Engineering*, **114**, 52—57.

DURST, F., MILOJEVIC, D. and SCHONUNG, B., (1984), "Eulerian and Lagrangian predictions of particle two-phase flows: A numerical study", *Applied Mathematical Modeling*, **8**, 101—115.

FINNIE, I., and McFADDEN, D.H., (1978), "On the velocity dependence of the erosion of ductile metals by solid particles at low angles of impingement", *Wear*, **48**, 181—190.

FINNIE, I., STEVICK, G.R., and RIDGELY, J.R., (1992), "The influence of impingement angle on the erosion of ductile metals by angular abrasive particles", *Wear*, **152**, 91—98.

FINNIE, I., WOLAK, J. and CABIL, Y., (1967), "Erosion of metals by solid particles", *Journal of Materials*, **2**, 682—700.

KAYS, W.M., and CRAWFORD, M.E., (1980), *Convective Heat and Mass Transfer*, McGraw-Hill.

KEATING, A., (1999), *A model for the investigation of two-phase erosion-corrosion in complex geometries*, Masters thesis, University of Queensland, Australia.

LAM, C.K.G. and BREMHORST, K., (1981), "A modified form of the k-ε model for predicting wall turbulence", *ASME Journal of Fluids Engineering*, **103**, 456—460.

LEONARD, B.P., (1979), "A stable and accurate convection modeling procedure based on quadratic upstream interpolation", *Computer Methods in Applied Mechanics and Engineering*, **19**, 59—98.

MAXEY, M.R., (1993), "The equation of motion for a small rigid sphere in a nonuniform or unsteady flow", *ASME/FED Gas-Solid Flows*, **166**, 57—62.

MILOJEVIC, D., (1990), "Lagrangian stochastic-deterministic (LSD) predictions of particle dispersion in turbulence", *Part. Part. Sys. Charact.*, **7**, 181—190.

NESIC, S., (1991), *Computation of localized erosion-corrosion in disturbed two-phase flow*, PhD thesis, University of Saskatchewan, Canada.

NESIC, S. and POSTLETHWAITE, J., (1991), "Hydrodynamic of disturbed flow and erosion-corrosion. Part I. Single-phase flow study", *The Canadian Journal of Chemical Engineering*, **69**, 693—703.

NESIC, S., POSTLETHWAITE, J. and BERGSTROM, D.J., (1992), "Calculation of wall mass transfer rates in seperated aqueous flow using a low Reynolds number k-ε model", *International Journal of Heat and Mass Transfer*, **35**, 1977—1985.

NOKLEBERG, L. and SONTVEDT, T., (1998), "Erosion of oil and gas industry choke valves using computational fluid dynamics and experiment", *International Journal of Heat and Fluid Flow*, **19**, 636—643.

PATANKAR, S.V. and SPALDING, D.B., (1972), "A calculation procedure for heat, mass and momentum transfer in three-dimensional parabolic flows", *International Journal of Heat and Mass Transfer*, **15**, 1787—1806.

WANG, J., SHIRAZI, S.A., SHADLEY, J.R., and RYBICKI, E.F., (1996), "Application of flow modeling and particle tracking to predict sand erosion rates in 90 degree elbows", *FED-Vol. 236, 1996 Fluids Engineering Division Conference*, 1, 725—734.